





Double-diffusive viscous fingering induced by an active dye

Y. Nagatsu¹  and A. De Wit² 

¹Department of Chemical Engineering, Tokyo University of Agriculture and Technology, 2-24-16 Naka-cho, Koganei, Tokyo 184-8588, Japan

²Nonlinear Physical Chemistry Unit, CP231, Université libre de Bruxelles (ULB), 1050 Brussels, Belgium

Corresponding author: A. De Wit, anne.de.wit@ulb.be

(Received 24 April 2025; revised 9 June 2025; accepted 19 June 2025)

Viscous fingering is a hydrodynamic instability typically occurring when a less viscous fluid displaces a more viscous one and which deforms the interface between the two fluids into finger-shaped intrusions. For miscible fluids, the fingering pattern is usually followed visually by adding a passive dye into one of the two fluids. The reverse displacement of a less viscous fluid by a more viscous one is classically stable, featuring a planar interface. Here, we show experimentally that in some cases, the dye can actively modify the viscosity of a polymer solution and trigger fingering in the reverse displacement. This dye-induced destabilisation is shown to be due to double-diffusive effects triggering a non-monotonic viscosity profile with a maximum because the dye diffuses faster than the polymer.

Key words: Hele-Shaw flows, coupled diffusion and flow, convection in porous media

1. Introduction

When a less viscous fluid displaces a more viscous one in porous media, the interface between the two fluids forms a finger-like pattern due to a viscous fingering (VF) or Saffman–Taylor instability (Saffman & Taylor 1958; Homsy 1987). Such VF has received a lot of attention because of its importance in various fields such as secondary and tertiary oil recovery (Tchelepi & Orr 1994), chromatographic separation (Broyles *et al.* 1998; Haudin *et al.* 2016), and even medical applications (Bhaskar *et al.* 1992).

Chemical reactions have been shown to affect VF when they modify *in situ* the interfacial tension for immiscible fluids (Fernandez & Homsy 2003) or viscosity in miscible interfaces (De Wit & Homsy 1999; Nagatsu *et al.* 2007, 2009; Hejazi *et al.* 2010*a*; Bunton *et al.* 2017; De Wit 2020; Escala & Muñozuri 2021; Tafur *et al.* 2021). As VF is usually a negative factor in terms of displacement efficiency, attention has also been paid to strategies for VF suppression via variable fluid injection rate

(Dias *et al.* 2012), reactors with an elastic membrane (Pihler-Puzovic *et al.* 2012), or gradients of permeability (Al-Housseiny, Tsai & Stone 2012), for instance.

Classically, in the reverse displacement, i.e. when the more viscous fluid displaces the less viscous one, the interface is stable with regard to VF, and remains planar. However, in some peculiar reverse cases, fingering can nevertheless develop. For immiscible systems, fingering of the interface has been observed in the reverse situation, driven by Marangoni effects (Chan & Liang 1997; Krechetnikov & Homsy 2004) or accumulation of suspensions (Tang *et al.* 2000), for instance. In the case of partially miscible interfaces, destabilisation of reverse displacements can be triggered by spinodal decomposition (Suzuki *et al.* 2019).

For miscible systems, Podgorski *et al.* (2007) demonstrated experimentally VF induced by a chemical reaction in the case of an aqueous reactant solution displacing another reactant solution of the same viscosity in a Hele-Shaw cell. The chemical reaction taking place in the contact zone between the two solutions produces a micellar material with viscoelastic properties, and fingering is then observed. Similar fingering between aqueous solutions of the same viscosity due to a precipitation reaction was reported by Nagatsu *et al.* (2014). In this case, the local change in permeability is the source of the fingering. Possibility of destabilisation by a chemical reaction of a reverse miscible displacement has been suggested theoretically to occur if non-monotonic viscosity profiles develop because of a reaction inducing locally either a maximum or a minimum in viscosity (Hejazi *et al.* 2010a). Nonlinear simulations show that fingering develops then at the back of the maximum where the less viscous injected solution crashes into the zone of maximum viscosity, while forward fingering is rather obtained ahead of a minimum (Hejazi & Azaiez 2010b,c; Nagatsu & De Wit 2011; Sharma *et al.* 2019). Experimental demonstration of both types of reaction-induced reverse fingering has been subsequently obtained using viscous polymer solutions displacing less viscous aqueous solutions of reactants (Riolfo *et al.* 2012; Escala *et al.* 2019; Escala & Muñuzuri 2021). Recent works have shown that reverse fingering can also be obtained in nanocatalytic reactive flows where the presence of nanocatalysts can affect the viscosity distribution (Dastvareh, Azaiez & Tsai 2019). In absence of reactions, reverse miscible fingering can further be obtained by non-ideal mixing effects of separate pure fluids triggering a local maximum in viscosity, as observed experimentally in displacements in micro-pillar arrays (Haudin *et al.* 2016).

Theoretically, double-diffusion has also been shown to be able to trigger VF in the reverse situation if the system involves two scalars that both affect viscosity independently, and diffuse at different rates (Pritchard 2009; Mishra *et al.* 2010). Such double-diffusion effects can occur typically due to differences in diffusivity of heat and mass in porous media, where they can then trigger also different convective speeds (Azaiez & Sajjadi 2012). More generally, the presence of two solutes affecting viscosity independently and having different diffusion coefficients is predicted to destabilise reverse displacements and yield new types of fingered patterns (Mishra *et al.* 2010). Such pure double-diffusion-induced VF has, however, not been evidenced yet experimentally.

In this context, we evidence here experimentally a novel mechanism of VF destabilisation of a reverse miscible displacement in the case of a dyed, viscous polymer solution displacing water in the absence of any chemical reaction. Contrary to what is usually hypothesised, the dye is here actively decreasing the viscosity of the polymer solution, even if present in a minute quantity. This viscosity reduction coupled to differential diffusion of the polymer and of the dye induces a non-monotonic viscosity profile with a maximum at the origin of the fingering pattern.

We first present the experimental observation of reverse VF, and then proceed with viscosity measurements and theoretical reconstruction of viscosity profiles to explain the

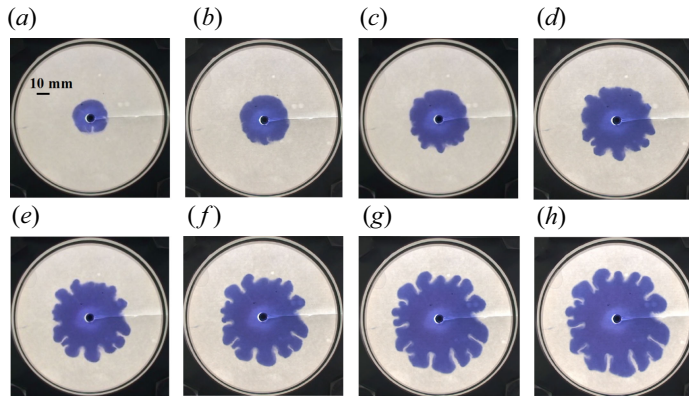


Figure 1. Fingering pattern formed when a solution of 0.5 wt % PAA (MW = 1.25 million) and 0.1 wt % TB displaces water for $Pe = 1.6 \times 10^3$ and $b = 0.3$ mm at (a) $t = 60$ s, $R = 15$ mm, (b) $t = 120$ s, $R = 20$ mm, (c) $t = 180$ s, $R = 26$ mm, (d) $t = 240$ s, $R = 33$ mm, (e) $t = 300$ s, $R = 35$ mm, (f) $t = 360$ s, $R = 40$ mm, (g) $t = 450$ s, $R = 44$ mm, and (h) $t = 510$ s, $R = 48$ mm.

origin of the VF of the reverse displacement. Our results not only introduce a novel way to destabilise a reverse displacement of a less viscous solution by a more viscous one, they also present the first experimental evidence of an active role of a dye and of differential diffusion effects in VF dynamics.

2. Dye-induced VF

Experiments are conducted in a Hele-Shaw cell consisting of two parallel horizontal plates separated by a small gap $b = 0.3$ mm in which radial displacements of one fluid by another miscible one of different viscosity are studied (Nagatsu *et al.* 2007). The less viscous fluid is here pure water, while the more viscous fluid is a solution of PAA (poly(acrylic acid) polymer from Aldrich, molecular weight (MW) 1.25 million) in concentration 0.5 wt %, mixed with Trypan Blue (TB) in concentration 0.1 wt %, a dye used for the visualisation of the pattern. For radial displacements in miscible systems, the Péclet number Pe is defined as $Pe = q/2\pi bD$ (Petitjeans *et al.* 1999; Nagatsu *et al.* 2007), where q is the injection rate of the displacing fluid, and D is the diffusion coefficient, which we estimate to be equal to $1 \times 10^{-9} \text{ m}^2 \text{ s}^{-1}$, a representative value of D for chemical species in water. Here, the flow rate is constant and fixed at $q = 3.0 \times 10^{-9} \text{ m}^3 \text{ s}^{-1}$, which gives $Pe = 1.6 \times 10^3$. The shear rate at the finger tip can be estimated as $\dot{\gamma}_f = q/\pi Rb^2$ (Vlad & Maher 2000; Nagatsu *et al.* 2007), where R is the radius of a stable displacement circle. In the present reactor, R is varied in the range $2 \text{ mm} \leq R \leq 58 \text{ mm}$, which leads to $0.2 \text{ s}^{-1} \leq \dot{\gamma}_f \leq 5 \text{ s}^{-1}$.

Figure 1 shows the temporal evolution of the displacement pattern when the more viscous dyed aqueous solution of PAA displaces water radially. Such a displacement of a less viscous fluid by a more viscous one is classically expected to be stable and hence feature a radially growing undeformed circular displacement. Yet a fingered deformation of the miscible interface, the amplitude of which grows in time, is clearly observed.

We emphasise that there is no chemical reaction taking place here, and that the only involved solutes are PAA and TB. This unexpected reverse VF is not a pure double-diffusion mechanism as studied before theoretically Mishra *et al.* (2010) because the dye in itself does not change the viscosity of the water solvent when present alone. It is also different from reverse VF induced by non-ideal effects due to mixing of one fluid with

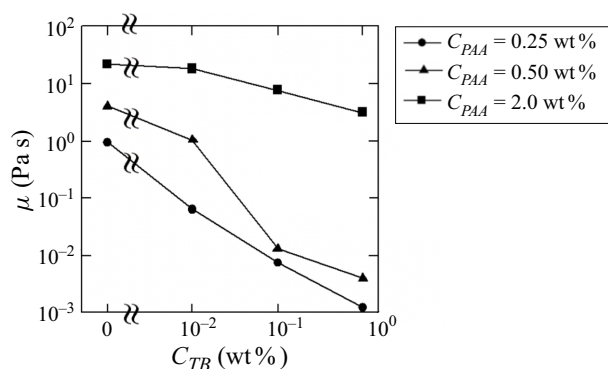


Figure 2. Viscosity of the solution of PAA (MW = 1.25 million) and TB in various concentrations at $\dot{\gamma} = 1 \text{ s}^{-1}$.

another (Haudin *et al.* 2016), as both the polymer and the dye are here initially present in the same solution, which is injected into water.

To clarify the origin of the instability, we have investigated the dependence of the solution's viscosity on the concentration of PAA and TB, using a rheometer (AR-G2, TA Instruments). First, the polymer solution has a shear-thinning viscosity behaviour, i.e. its viscosity decreases when the shear rate increases. Figure 2 shows the viscosity as a function of the TB concentration for three different concentrations of PAA at a fixed shear rate of 1 s^{-1} , a value chosen because it corresponds to the shear rate at approximately $R = 10\text{--}15 \text{ mm}$ where the instability starts to develop (see figure 1a). The solution's viscosity increases with the concentration of the polymer, which is quite classical. An unexpected trend is, however, that the dye is not passive here. On the contrary, the viscosity of each polymer solution decreases when the amount of TB increases, even if this amount is very small (less than 1 %). The dye plays here clearly an active role, and the viscosity of the solution depends on the simultaneous presence of both the polymer and the dye. The active role of TB is due to the fact that the addition of metal ions to an aqueous solution of anionic polymers reduces the solution viscosity (Escala *et al.* 2017; Escala *et al.* 2019; Tam & Tiu 1990). In the aqueous solutions used here, positively charged Na^+ sodium ions are released by TB, while PAA behaves as an anionic polymer as many of the side chains of PAA lose their protons in water to become negatively charged. When the concentration of metal ions is sufficiently high, the electrostatic field established by the anionic polymer is screened out, and the apparent size of the polymer in solution becomes smaller, which leads to a decrease in the solution viscosity. Note that in absence of PAA, the viscosity of the dyed water is simply the viscosity of pure water, unaffected by the presence of the dye.

3. Viscosity profiles

Previous works on reactive systems have shown that the destabilisation of the displacement of a less viscous fluid by a more viscous one can occur when a non-monotonic viscosity profile builds up thanks to the reaction changing the viscosity *in situ* (Hejazi *et al.* 2010a; Riolfo *et al.* 2012). Here, there is no reaction, but the viscosity of the polymer solution decreases in the presence of TB. We will seek to understand how the spatial distribution of the viscosity varies in our system when PAA and TB are initially dissolved in the same solution but diffuse at different rates. As it is difficult to measure quantitatively the viscosity field *in situ* during the displacement (Bunton *et al.* 2016a,b), we resort to reconstructing one-dimensional (1-D) viscosity profiles on the basis of 1-D analytical concentration profiles (Riolfo *et al.* 2012).

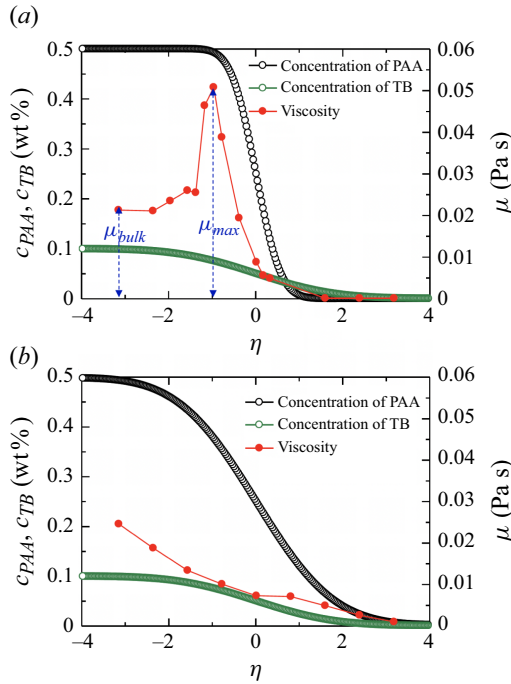


Figure 3. Concentration profiles of PAA and TB, and reconstructed viscosity profiles computed for 0.5 wt % PAA (MW = 1.25 million) and 0.1 wt % TB, as studied in figure 1 when (a) $\delta = 10$, (b) $\delta = 1$.

Considering that in absence of fingering we have transverse symmetry, and assuming a constant velocity, the 1-D concentration profiles $c_{PAA}(x, t)$ and $c_{TB}(x, t)$ for PAA and TB, respectively, can be computed as solutions of Fick's law of diffusion:

$$\frac{\partial c_{PAA}}{\partial t} = D_{PAA} \frac{\partial^2 c_{PAA}}{\partial x^2}, \tag{3.1}$$

$$\frac{\partial c_{TB}}{\partial t} = D_{TB} \frac{\partial^2 c_{TB}}{\partial x^2}. \tag{3.2}$$

We consider a solution of PAA at initial concentration $c_{PAA}^0 = 0.5\%$ containing TB at an initial concentration $c_{TB}^0 = 0.1\%$ so that the base state solutions for PAA and TB are

$$c_{PAA} = \frac{c_{PAA}^0}{2} \operatorname{erfc}(\eta) \quad \text{and} \quad c_{TB} = \frac{c_{TB}^0}{2} \operatorname{erfc}(\eta/\sqrt{\delta}), \tag{3.3}$$

where $\eta = x/\sqrt{4D_{PAA}t}$ and $\delta = D_{TB}/D_{PAA}$. These profiles are plotted in figures 3(a) and 3(b) for different and equal diffusion coefficients, respectively. Thanks to these concentration profiles, the spatial variation of the base state viscosity profile can be reconstructed. In practice, we select a dozen locations in space where the concentration of each species is known. Then we prepare in separate beakers a mixture of PAA and TP in the relevant proportions, and measure the viscosity of the solution by a rheometer as a function of the shear rate. The viscosities at the shear rate 1 s^{-1} are then used to reconstruct the 1-D spatial profile of viscosity in figure 3.

Figure 3(a) focuses on the case where δ is larger than 1. This assumption is reasonable as the polymer is a macromolecule that diffuses slower than the dye molecule, which has a much lower molecular weight. Here, we assume that the value of the diffusivities differ by

one order of magnitude, i.e. $\delta = 10$. Figure 3(b) shows the profiles for equal diffusivities of PAA and TB ($\delta = 1$). We see that when TB diffuses faster than PAA, a non-monotonic spatial variation of the viscosity is obtained, i.e. the viscosity presents a maximum along the displacement direction, while the viscosity varies monotonically in space in the equal diffusion case. In figure 3(a), the local maximum develops around $\eta = -1$ where c_{PAA} is still very close to its initial value $c_{PAA}^0 = 0.5\%$, while the concentration of TB has dropped to approximately 80% of its bulk value $c_{TB}^0 = 0.1\%$ because TB diffuses faster than PAA. In comparison, around $\eta = -3$, the decrease in viscosity is larger because the concentration of TB is still larger as well. Much further downstream, i.e. for $\eta > 0$, the concentration of polymer has dropped so that the viscosity becomes very low again. This leads to the presence of a local maximum in viscosity at intermediate regions of the profile. In figure 3(b) with $\delta = 1$, the viscosity profile is monotonically decreasing because the ratio of the concentrations of PAA and TB is the same everywhere since the diffusivity of PAA and TB is the same. We note that for this value of shear rate (1 s^{-1}), elastic effects of the 0.5 wt % PAA solutions can be neglected, as confirmed by measurements of the first normal stress difference (Nagatsu *et al.* 2007).

A careful analysis thus shows that the non-monotonic profile is possible thanks to the combination of three ingredients: (i) PAA increases the viscosity; (ii) TB decreases the viscosity of the PAA solution; and (iii) TB diffuses faster than PAA.

4. Parametric study

To further clarify the origin of the VF instability shown in figure 1, we have conducted a parametric study varying the concentrations of PAA and TB, keeping the injection rate constant. Figure 4(a) shows the displacement pattern for the same TB concentration as in figure 1 but a larger PAA concentration, while figure 4(b) features the displacement for the same PAA concentration as in figure 1 but a lower amount of dye. Note that the blue colour is here lighter because the dye concentration is smaller. In both cases, VF hardly occurs.

To understand why VF disappears for the experimental values of parameters considered in figure 4, we have reconstructed the viscosity profiles for those conditions using the methodology described above, assuming $\delta = 10$. Figures 5(a) and 5(b) show the viscosity profiles corresponding to the values of parameters of figures 4(a) and 4(b), respectively. In both cases, the viscosity profiles still exhibit a non-monotonic behaviour, but the amplitude of the maximum is much smaller than in the unstable case of figure 3. To appreciate this, let us compare the viscosity of the displacing fluid denoted μ_{bulk} to the viscosity of the local maximum μ_{max} . Note that here the displaced less viscous fluid is always water, the viscosity of which is minimal. In the stable cases of figures 4 and 5, the ratio μ_{max}/μ_{bulk} is roughly equal to 1.1–1.3, while it is closer to 2.4 in the unstable dynamics corresponding to figures 1 and 3(a). These results suggest that the instability is indeed triggered by the extremum in viscosity but that its amplitude should exceed a given threshold to induce the destabilisation. Note that figure 1 shows that the effect of the dye on the viscosity of PAA is strongest for $c_{PAA} = 0.5\text{ wt}\%$ and c_{TB} in the range 0.01–0.1 wt %, which are the values of parameters for which we get the highest μ_{max}/μ_{bulk} shown in figure 3(a). The less strong change of the viscosity of PAA on the dye for $c_{PAA} = 0.5\text{ wt}\%$ in the regimes where $c_{TB} < 0.01\text{ wt}\%$ or $c_{TB} > 0.1\text{ wt}\%$ results in the lower μ_{max}/μ_{bulk} shown in figure 5(b). The amplitude of this μ_{max}/μ_{bulk} ratio is thus a subtle function of both c_{PAA} and c_{TB} in addition to the value of δ . Note that for shear rate 1 s^{-1} , measurements of the first normal stress difference as in Nagatsu *et al.* (2007) show that elastic effects of the 2 wt % PAA solution cannot be neglected. However, as elastic effects of the 0.5 wt %

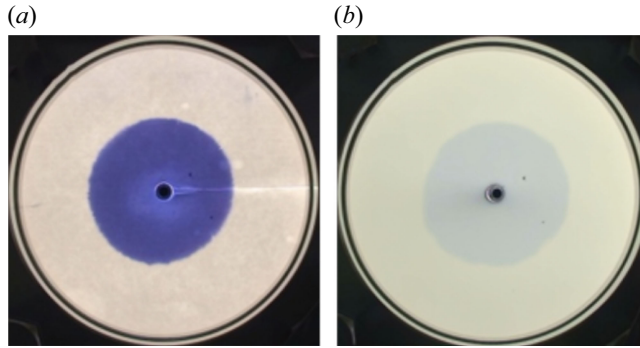


Figure 4. Displacement patterns at $t = 300$ s observed when a solution of PAA (MW = 1.25 million) and TB in various concentrations displaces water for $Pe = 1.6 \times 10^3$ and $b = 0.3$ mm: (a) $C_{PAA} = 2$ wt % and $C_{TB} = 0.1$ wt %; (b) $C_{PAA} = 0.5$ wt % and $C_{TB} = 0.01$ wt %.

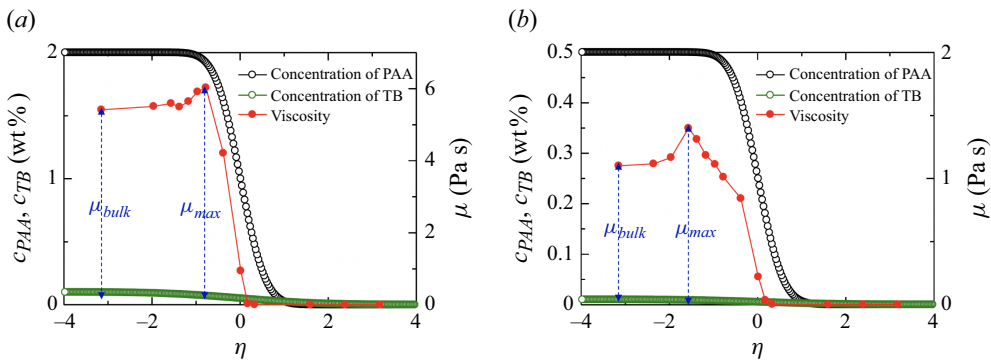


Figure 5. Concentration and viscosity profiles computed using $\delta = 10$ and the values of parameters of (a) figure 4(a) and (b) figure 4(b).

PAA solution can be neglected, such elastic effects should not be responsible for the disappearance of the fingering.

The fact that the viscosity of the injected solution depends on two chemical species is a key prerequisite here to obtain a local extremum in its spatial profile. If the viscosity of the PAA solution becomes independent of the presence of TB, then the viscosity can only monotonically decrease along the displacement. To show this, we have repeated the experiments with a solution of PAA with a much smaller molecular weight (0.25 million, PAA from Wako, Japan) and larger concentrations of 2.0 and 4.0 wt %. As shown in figure 6, in that case the viscosity of the polymer does not vary when the TB dye is added. In that case, only monotonic decreasing viscosity profiles can build up, and no VF instability is observed, as seen in figure 7. This confirms that the destabilisation of the reverse displacement shown in figure 1 is obtained for some PAA of sufficient molecular weight for which the dye affects its viscosity.

For future possible modelling, we note that our system is different from the pure double-diffusive case of Mishra *et al.* (2010) where the viscosity is modelled as $\mu = \exp [R_s S + R_f F]$, with S and F the concentrations of the slow and fast species, respectively, and R_s , R_f the constant log-mobility ratios. In their case, each species influences the viscosity of the solution independently of the other one. In the PAA/TB system presented here, the state equation of viscosity as a function of the concentration of $A = \text{PAA}$ and $B = \text{TB}$ is

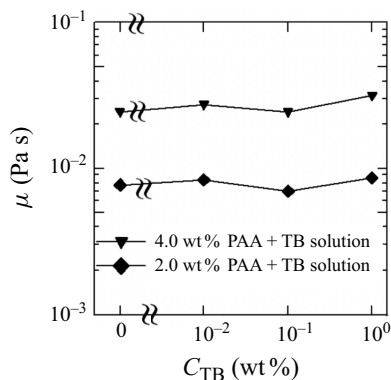


Figure 6. Viscosities of the 2.0 and 4.0 wt % solutions of PAA (MW = 0.25 million) as functions of the concentration of TB, measured at $\dot{\gamma} = 1 \text{ s}^{-1}$.

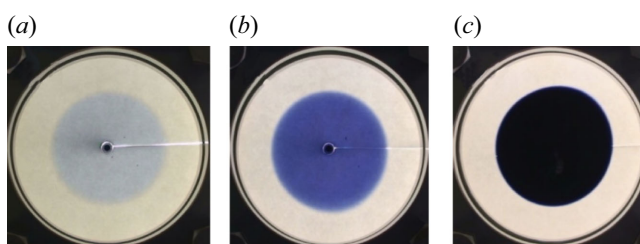


Figure 7. Displacement patterns observed at $t = 300 \text{ s}$ for $Pe = 1.6 \times 10^3$ and $b = 0.3 \text{ mm}$ when water is displaced by a 4.0 wt % solution of PAA (MW = 0.25 million) containing TB in concentration (a) 0.01 wt %, (b) 0.1 wt %, (c) 1 wt %.

more complex and probably of the type $\mu = \exp[R(B)A]$ such that TB alone does not change the viscosity of water, but the log-mobility ratio R in the viscosity of the PAA solution varies with the concentration B of TB.

5. Conclusions

In conclusion, we have experimentally demonstrated viscous fingering (VF) of a reverse displacement of water by a more viscous solution of a poly(acrylic acid) (PAA) polymer dyed by Trypan Blue (TB) in a Hele-Shaw cell. Classically such a displacement is supposed to induce a circular displacement because the more viscous fluid is injected into the less viscous one, a hydrodynamically stable case. Yet we have shown that for PAA of sufficiently large molecular weight, a clear fingered pattern is obtained. The instability here is not due to a reaction as the displaced solution is pure water. A pure double-diffusion VF involving two solutes changing independently the viscosity as analysed by Mishra *et al.* (2010) is also not at play as the TB dye alone does not change the viscosity of water. Non-ideal mixing effects between two solutes initially separated, as studied by Haudin *et al.* (2016), are also not relevant as the dye and the polymer are initially present in the same displacing fluid.

To clarify the origin of the instability, we have shown that the polymer solution's viscosity increases with the concentration of PAA, whereas it decreases with that of TB. The viscosity profile has been reconstructed based on the concentration profiles of PAA and TB obtained from one-dimensional diffusion equations. If the polymer and the dye

are assumed to diffuse at the same rate, then the viscosity profile remains monotonically decreasing, and no instability can develop. However, if the dye is assumed to diffuse faster than the long chain polymer, then the viscosity profile is non-monotonic with a local maximum. If the ratio of the local maximum viscosity to the viscosity of the displacing solution is sufficiently large, then a reverse VF instability is observed. However, when the ratio is small, the VF instability hardly occurs.

These results show that reverse VF is here obtained as a combination of a change in the viscosity of a polymer solution due to the presence of a dye, and double-diffusive effects. While the potential active role of dyes has already been evidenced in buoyancy-driven flows (Kuster *et al.* 2011), we have evidenced here for the first time its active role in triggering a viscous instability, inviting us therefore to use dyes with caution in future experiments on viscous effects. Our results are also the first experimental evidence of a VF instability triggered by differential diffusion effects, which paves the way to analyse new fingering dynamics using solutions containing more than one solute.

Acknowledgements. We thank S. Iwata and L. Riolfo for conducting preliminary experiments, and Y. Tada, P.M.J. Trevelyan and D. Escala for fruitful discussions.

Funding. Y.N. acknowledges the financial support of KAKENHI from the Japan Society for the Promotion of Science (JSPS) (grant no. 22686020). A.D. acknowledges the financial support of the FRS-FNRS PHYLLLO project and of PRODEX. We both gratefully acknowledge the Institute of Global Innovation research of TUAT for supporting financially our bilateral collaboration.

Declaration of interests. The authors report no conflict of interest.

REFERENCES

- AL-HOUSSEINY, T.T., TSAI, P.A. & STONE, H.A. 2012 Control of interfacial instabilities using flow geometry. *Nat. Phys.* **8** (10), 747–750.
- AZAIÉZ, J. & SAJJADI, M. 2012 Stability of double-diffusive double-convective miscible displacements in porous media. *Phys. Rev. E* **85** (2), 026306.
- BHASKAR, K.R., GARIK, P., TURNER, B.S., BRADLEY, J.D., BANSIL, R., STANLEY, H.E. & LAMONT, J.T. 1992 Viscous fingering of HCl through gastric mucin. *Nature* **360** (6403), 458–461.
- BROYLES, B.S., SHALLIKER, R.A., CHERRAK, D.E. & GUIOCHON, G. 1998 Visualization of viscous fingering in chromatographic columns. *J. Chromatogr. A* **822** (2), 173–187.
- BUNTON, P., DICE, B., POJMAN, J.A., DE WIT, A. & BRAU, F. 2016a Reconstruction by fluorescence imaging of the spatio-temporal evolution of the viscosity field in Hele-Shaw flows. *Phys. Fluids* **26** (11), 114106.
- BUNTON, P., MARIN, D., STEWART, S., MEIBURG, E. & DE WIT, A. 2016b Schlieren imaging of viscous fingering in a horizontal Hele-Shaw cell. *Exp. Fluids* **57**, 28.
- BUNTON, P., TULLIER, M.P., MEIBURG, E. & POJMAN, J.A. 2017 The effect of a crosslinking chemical reaction on pattern formation in viscous fingering of miscible fluids in a Hele-Shaw cell. *Chaos* **27** (10), 104614.
- CHAN, C.K. & LIANG, N.Y. 1997 Observations of surfactant driven instability in a Hele-Shaw cell. *Phys. Rev. Lett* **79** (22), 4381–4384.
- DASTVAREH, B., AZAIÉZ, J. & TSAI, P.A. 2019 Nanocatalytic chemo-hydrodynamic instability: deposition effects. *Phys. Rev. E* **100** (5), 053102.
- DE WIT, A. 2020 Chemo-hydrodynamic patterns and instabilities. *Annu. Rev. Fluid Mech.* **52** (1), 531–555.
- DE WIT, A. & HOMSY, G.M. 1999 Nonlinear interaction of chemical reactions and viscous fingering in porous media. *Phys. Fluids* **11** (5), 949–951.
- DIAS, E.O., ALVAREZ-LACALLE, E., CARVALHO, M.S. & MIRANDA, J.A. 2012 Minimization of viscous fluid fingering: a variational scheme for optimal flow rates. *Phys. Rev. Lett* **109** (14), 144502.
- ESCALA, D.M., DE WIT, A., CARBALLIDO-LANDEIRA, J. & MUÑUZURI, A.P. 2019 Viscous fingering induced by a pH-sensitive clock reaction. *Langmuir* **35**, 4182–4188.
- ESCALA, D.M. & MUÑUZURI, A.P. 2021 A bottom-up approach to construct or deconstruct a fluid instability. *Sci. Rep.*, **11**, 24368.

- ESCALA, D.M., MUÑUZURI, A.P., DE WIT, A. & CARBALLIDO-LANDEIRA, J. 2017 Temporal viscosity modulations driven by a pH sensitive polymer coupled to a pH-shifting chemical reaction. *Phys. Chem. Chem. Phys.* **19**, 11914–1191.
- FERNANDEZ, J. & HOMSY, G.M. 2003 Viscous fingering with chemical reaction: effect of in-situ production of surfactants. *J. Fluid Mech.*, **480**, 267–281.
- HAUDIN, F., CALLEWAERT, M., DE MALSCHE, W. & DE WIT, A. 2016 Influence of nonideal mixing properties on viscous fingering in micropillar array columns. *Phys. Rev. Fluids* **1** (7), 074001.
- HEJAZI, S.H. & AZAIEZ, J. 2010*b* Non-linear interactions of dynamic reactive interfaces in porous media. *Chem. Engng Sci.* **65** (2), 938–949.
- HEJAZI, S.H. & AZAIEZ, J. 2010*c* Hydrodynamic instability in the transport of miscible reactive slices through porous media. *Phys. Rev. E* **81** (5), 056321.
- HEJAZI, S.H., TREVELYAN, P.M.J., AZAIEZ, J. & DE WIT, A. 2010*a* Viscous fingering of a miscible reactive $A + B \rightarrow C$ interface: a linear stability analysis. *J. Fluid Mech.* **652**, 501–528.
- HOMSY, G.M. 1987 Viscous fingering in porous media. *Annu. Rev. Fluid Mech.* **19** (1), 271–311.
- KRECHETNIKOV, R. & HOMSY, G.M. 2004 On a new surfactant-driven fingering phenomenon in a Hele-Shaw cell. *J. Fluid Mech.* **509**, 103–124.
- KUSTER, S., RIOLFO, L.A., ZALTS, A., EL HASI, C., ALMARCHA, C., TREVELYAN, P.M.J., DE WIT, A. & D'ONOFRIO, A. 2011 Differential diffusion effects on buoyancy-driven instabilities of acid-base fronts: the case of a color indicator. *Phys. Chem. Chem. Phys.* **13** (38), 17295.
- MISHRA, M., TREVELYAN, P.M.J., ALMARCHA, C. & DE WIT, A. 2010 Influence of double diffusive effects on miscible viscous fingering. *Phys. Rev. Lett* **105** (20), 204501.
- NAGATSU, Y. & DE WIT, A. 2011 Viscous fingering of a miscible reactive $A + B \rightarrow C$ interface for an infinitely fast chemical reaction: nonlinear simulations. *Phys. Fluids* **23**, 043103.
- NAGATSU, Y., ISHII, Y., TADA, Y. & DE WIT, A. 2014 Hydrodynamic fingering instability induced by a precipitation reaction. *Phys. Rev. Lett.* **113** (2), 024502.
- NAGATSU, Y., KONDO, Y., KATO, Y. & TADA, Y. 2009 Effects of moderate Damköhler number on miscible viscous fingering involving viscosity decrease due to a chemical reaction. *J. Fluid Mech.* **625**, 97–124.
- NAGATSU, Y., MATSUDA, K., KATO, Y. & TADA, Y. 2007 Experimental study on miscible viscous fingering involving viscosity changes induced by variations in chemical species concentrations due to chemical reactions. *J. Fluid Mech.* **571**, 475–493.
- PETITJEANS, P., CHEN, C.Y., MEIBURG, E. & MAXWORTHY, T. 1999 Miscible quarter five-spot displacements in a Hele-Shaw cell and the role of flow-induced dispersion. *Phys. Fluids* **11** (7), 1705–1716.
- PIHLER-PUZOVIC, D., ILLIEN, P., HEIL, M. & JUEL, A. 2012 Suppression of complex fingerlike patterns at the interface between air and a viscous fluid by elastic membranes. *Phys. Rev. Lett.* **108** (7), 074502.
- PODGORSKI, T., SOSTARECZ, M.C., ZORMAN, S. & BELMONTE, A. 2007 Fingering instabilities of a reactive micellar interface. *Phys. Rev. E* **76** (1), 016202.
- PRITCHARD, D. 2009 The linear stability of double-diffusive miscible rectilinear displacements in a Hele-Shaw cell. *Eur. J. Mech. B/Fluids* **28** (4), 564–577.
- RIOLFO, L.A., NAGATSU, Y., IWATA, S., MAES, R., TREVELYAN, P.M.J. & DE WIT, A. 2012 Experimental evidence of reaction-driven miscible viscous fingering. *Phys. Rev. E* **85** (1), 015304(R).
- SAFFMAN, P.G. & TAYLOR, G.I. 1958 The penetration of a fluid into a porous medium or Hele-Shaw cell containing a more viscous liquid. *Proc. R. Soc. Lond. A* **245** (1242), 312–329.
- SHARMA, V., PRAMANIK, S., CHEN, C.-Y. & MISHRA, M. 2019 A numerical study on reaction-induced radial fingering instability. *J. Fluid Mech.* **862**, 624–638.
- SUZUKI, R.X., NAGATSU, Y., MISHRA, M. & BAN, T. 2019 Fingering pattern induced by spinodal decomposition in hydrodynamically stable displacement in a partially miscible system. *Phys. Rev. Fluids* **4** (10), 104005.
- TAFUR, N., ESCALA, D.M., SOTO, A. & MUÑUZURI, A.P. 2021 Highly viscous fluid displaced by a chemically controlled reactive interface. *Chaos* **31** (2), 023135.
- TAM, K.C. & TIU, C. 1990 Role of ionic species and valency on the steady shear behavior of partially hydrolyzed polyacrylamide solutions. *Colloid Polym. Sci.* **268** (10), 911–920.
- TANG, H., GRIVAS, W., HOMENTCOVSCHI, D., GEER, J. & SINGLER, T. 2000 Stability considerations associated with the meniscoid particle band at advancing interfaces in Hele-Shaw suspension flows. *Phys. Rev. Lett* **85** (10), 2112–2115.
- TCHELEPI, H.A. & ORR, F.M. 1994 Interaction of viscous fingering, permeability heterogeneity, and gravity segregation in three dimensions. *SPE Reservoir Engng* **9** (4), 266–271.
- VLAD, D.H. & MAHER, J.V. 2000 Tip-splitting instabilities in the channel Saffman–Taylor flow of constant viscosity elastic fluids. *Phys. Rev. E* **61** (5), 5439–5444.